



Nonlinear optical properties of Bi₂O₃-GeO₂ glass at 800 and 532nm

Tâmara R. Oliveira, Edilson L. Falcão-Filho, Cid B. de Araújo, Diego S. da Silva, Luciana R. P. Kassab, and Davinson M. da Silva

Citation: [Journal of Applied Physics](#) **114**, 073503 (2013); doi: 10.1063/1.4818502

View online: <http://dx.doi.org/10.1063/1.4818502>

View Table of Contents: <http://scitation.aip.org/content/aip/journal/jap/114/7?ver=pdfcov>

Published by the [AIP Publishing](#)



Re-register for Table of Content Alerts

Create a profile.



Sign up today!



Nonlinear optical properties of Bi₂O₃-GeO₂ glass at 800 and 532 nm

Tâmara R. Oliveira,¹ Edilson L. Falcão-Filho,² Cid B. de Araújo,^{2,a)} Diego S. da Silva,³ Luciana R. P. Kassab,⁴ and Davinson M. da Silva⁴

¹Departamento de Física, Universidade Estadual da Paraíba, 58429-500 Campina Grande, PB, Brazil

²Departamento de Física, Universidade Federal de Pernambuco, 50670-901 Recife, PE, Brazil

³Departamento de Engenharia de Sistemas Eletrônicos, Escola Politécnica, Universidade de São Paulo, 05508-970 São Paulo, SP, Brazil

⁴Laboratório de Tecnologia em Materiais Fotônicos e Optoeletrônicos, Faculdade de Tecnologia de São Paulo, CEETEPS/UNESP, 01124-060 São Paulo, SP, Brazil

(Received 2 June 2013; accepted 31 July 2013; published online 16 August 2013)

The nonlinear (NL) optical properties of glassy $x\text{Bi}_2\text{O}_3-(1-x)\text{GeO}_2$ with $x=0.72$ and 0.82 were investigated. The experiments were performed with lasers at 800 nm (pulses of 150 fs) and 532 nm (pulses of 80 ps and 250 ns). Using the Kerr gate technique, we observed that the NL response of the samples at 800 nm is faster than 150 fs. NL refractive indices, $|n_2| \approx 5 \times 10^{-16} \text{ cm}^2/\text{W}$, and two-photon absorption coefficients, α_2 , smaller than $0.03 \text{ cm}/\text{GW}$, were measured at 800 nm. At 532 nm, we measured the NL transmittance of the samples. From the results obtained, we determined $\alpha_2 \approx 1 \text{ cm}/\text{GW}$ and excited-state absorption cross-sections of $\approx 10^{-22} \text{ cm}^2$ due to free-carriers. © 2013 AIP Publishing LLC. [<http://dx.doi.org/10.1063/1.4818502>]

I. INTRODUCTION

Glassy materials for nonlinear (NL) photonics have been intensively studied in the past years. In particular, there is great interest in glasses based on heavy-metal oxides (HMO) because they present large NL behavior, high transmittance in the near-infrared and visible, large chemical durability, and good temperature stability. The large third-order optical susceptibility, $\chi^{(3)}$, due to the high polarizability of the heavy-metal ions, allows applications of HMO glasses in optical limiting, optical amplifiers, and all-optical switching.¹⁻¹²

The HMO glasses containing bismuth oxide, Bi₂O₃, present large nonlinearity because of the high polarizability of the Bi³⁺ ion due to its lone-electron pair in the valence shell and its large ionic radius. Moreover, with the introduction of Bi₂O₃ in a HMO glass network, the number of non-bridging oxygen grows, and thus, the optical refractive and absorptive properties of the material increase. The NL properties of glasses with Bi₂O₃ were discussed by various authors that report large NL refractive index and high two-photon absorption (TPA) coefficients for certain glass compositions.^{7-9,12-15} For instance, the influence of Bi₂O₃ on the structural, thermal, and NL optical properties of phosphate glasses was investigated recently.⁹ The results obtained show that the NL refractive indices increase with the increase of the Bi₂O₃ concentration.

Among the HMO glasses of interest Bi₂O₃-GeO₂ glass (labeled as BGO glass) was characterized with respect to its properties of photoluminescence (PL),¹⁶⁻²² optical amplification, and stimulated Raman.²⁰⁻²² The synthesis of this glass is simple and the results in the literature¹⁶⁻²² indicate that BGO glass is a good choice for photonic applications. Moreover, with basis on published results for the several

materials containing Bi₂O₃, we expect that BGO glass can also be used for NL photonics.

In this paper, we report on NL experiments with BGO glass at 800 nm and 532 nm. Optical response faster than 150 fs, NL refractive index of $\approx 5 \times 10^{-16} \text{ cm}^2/\text{W}$, and TPA coefficient, α_2 , smaller than $0.03 \text{ cm}/\text{GW}$ were measured at 800 nm. Experiments to measure α_2 at 532 nm with picosecond and nanosecond lasers were also performed. The results indicate that the BGO glass presents large TPA coefficient ($\approx 1 \text{ cm}/\text{GW}$) and free-carriers absorption cross-sections of $\approx 10^{-22} \text{ cm}^2$.

II. EXPERIMENTAL DETAILS

The samples were produced by the melting-quenching method using the starting compositions (in wt. %): 72Bi₂O₃-28GeO₂ (sample A) and 82Bi₂O₃-18GeO₂ (sample B). The reagents were melted in an alumina crucible for 1 h at 1100 °C, quenched in air inside a preheated brass mold, and annealed at 420 °C. Heat-treatment of the samples was performed to minimize internal stress. Finally, the samples were cut and polished for the optical measurements.

A commercial spectrophotometer was used to measure the linear optical absorption spectra of the samples. Two laser sources were used for the NL experiments. A mode-locked Ti-sapphire laser (800 nm, 76 MHz, 100 fs) was used for measurements based on the Kerr-gate technique.³ The second harmonic of a Q-switched and mode-locked Nd:YAG laser was used for measurements at 532 nm. Two laser configurations were used. In one configuration, single 80 ps pulses with repetition rate of 6 Hz were extracted from the pulse-train using an electro-optical switch (pulse-picker). In another experimental configuration, the pulse-picker was removed and the 250 ns Q-switch envelope containing 20 pulses of 80 ps separated by ≈ 13 ns was incident on the sample with repetition rate of 6 Hz. In both cases, the NL transmittance of the samples was measured using two

^{a)}Author to whom correspondence should be addressed. Electronic mail: cid@df.ufpe.br.

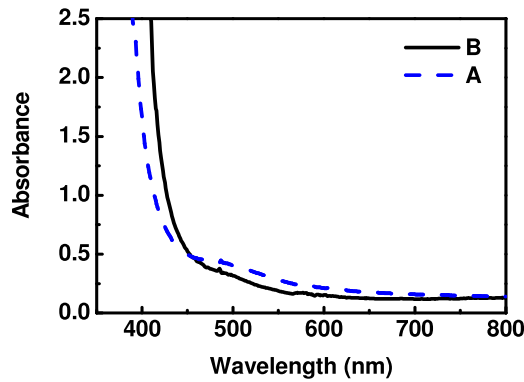


FIG. 1. Absorbance spectra. Samples' thicknesses: 2.1 mm (sample A); 2.0 mm (sample B).

photodiodes to determine the ratio between the transmitted and the incident laser intensity.

III. RESULTS AND DISCUSSIONS

Figure 1 shows the linear absorption spectra of the samples from the blue/green to the near-infrared. Notice that the short wavelength absorption-edge shifts to longer wavelengths when the Bi_2O_3 content is increased as it was already noticed for other glass compositions containing bismuth.^{23,24} The absorption-edge shift is attributed to the formation of non-bridging oxygen units that occurs when the bismuth oxide amount is increased.

The linear refractive indices and the linear absorption coefficients of the samples studied are given in Table I. The refraction index of samples A and B differ by $\approx 5\%$ which is about the ratio between the polarizabilities of the samples considering the relative amount of Bi_2O_3 and GeO_2 , in agreement with Ref. 25. We also notice that the linear absorption coefficient of sample B is smaller than the absorption coefficient of sample A, in accordance with Ref. 15, which shows that the absorption from the green to the near-infrared region is mainly due to the presence of GeO_2 .

The results of the NL experiments are described below for experiments performed with different excitation conditions.

A. Femtosecond nonlinearity at 800 nm

The NL response of the samples at 800 nm was investigated using the Kerr-gate technique.³ To perform the experiments, the laser beam was split in pump and probe beams with intensities of 1.2 GW/cm^2 and 120 MW/cm^2 , respectively. The sample was positioned between two crossed polarizers and the angle between the electric fields of the two incident beams was 45° . When the pulses of the two

TABLE I. Compositions and samples' parameters: d is the samples' length, n_0 is the linear index of refraction, and α_0 is the linear absorption coefficient.

Sample	Composition (% mol.)	D (mm)	n_0	α_0 (cm^{-1})		
				633 nm	532 nm	800 nm
A	$72\text{Bi}_2\text{O}_3\text{-}28\text{GeO}_2$	2.1	2.02	2.40	0.38	
B	$82\text{Bi}_2\text{O}_3\text{-}18\text{GeO}_2$	2.0	2.10	1.20	0.14	

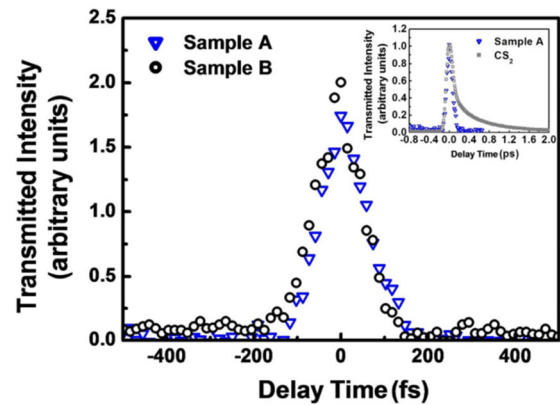


FIG. 2. Kerr gate signals for the two samples studied. The inset shows the Kerr signal for a cell with liquid CS_2 , our reference standard.

beams overlap spatially and temporally on the sample, the pump beam induces a NL birefringence that produces polarization rotation of the transmitted probe beam. The rotation mechanism is due to $\chi^{(3)}$ and the phase induced by the pump beam on the probe beam is given by $\phi_{NL} = 2\pi n_0 d n_2 I_P^2 / 3\lambda$, where I_P is the pump intensity, $n_0 d$ is the optical path inside the sample of thickness d , and λ is the optical wavelength.³ Due to the polarization rotation, a fraction of the probe beam is transmitted through a polarizer/analyzer, which is oriented perpendicularly to the electric field of the incident probe beam. The transmitted signal is analyzed as a function of the delay time between the pump and probe pulses.

Figure 2 shows the behavior of the normalized Kerr-gate signal as a function of delay time. The symmetric signals indicate that the samples' nonlinearity is faster than the laser pulse duration. CS_2 was used as a calibration standard with $n_2 = (3.1 \pm 1.0) \times 10^{-15} \text{ cm}^2/\text{W}$ (Ref. 26) to determine the samples' NL refractive indices that are indicated in Table II. The inset of Fig. 2 shows the signal corresponding to CS_2 with two decay times: a fast one ($< 50 \text{ fs}$) and a slow one of $\approx 2 \text{ ps}$ to illustrate the time resolution of the experimental setup.

Trials to determine α_2 in one-beam experiment measuring the transmitted intensity as a function of the incident beam intensity were unsuccessful indicating that α_2 is smaller than the minimum value that our setup can measure (0.03 cm/GW). Because the sensitivity of the setup used does not allow the precise measurement of the α_2 value, it is not possible to evaluate the potential of BGO for all-optical switching. The value of $\alpha_2 \lambda / n_2$ the figure-of-merit obtained would indicate possible use of BGO if the actual value of α_2 is at least smaller than 0.03 cm/GW by a factor 5.²⁷

TABLE II. Nonlinear parameters of the samples: $|n_2|$ is the modulus of the nonlinear refractive index, α_2 is the two-photon absorption coefficient, and σ_{FC} is the free-carriers absorption cross-section.

Sample	$ n_2 $ at 800 nm ($\times 10^{-16} \text{ cm}^2/\text{W}$)	α_2 at 532 nm (cm/GW)	σ_{FC} at 532 nm ($\times 10^{-22} \text{ cm}^2$)
A	5.4 ± 0.5	1.4 ± 0.3	1.9 ± 0.3
B	5.7 ± 0.6	1.1 ± 0.2	1.2 ± 0.3

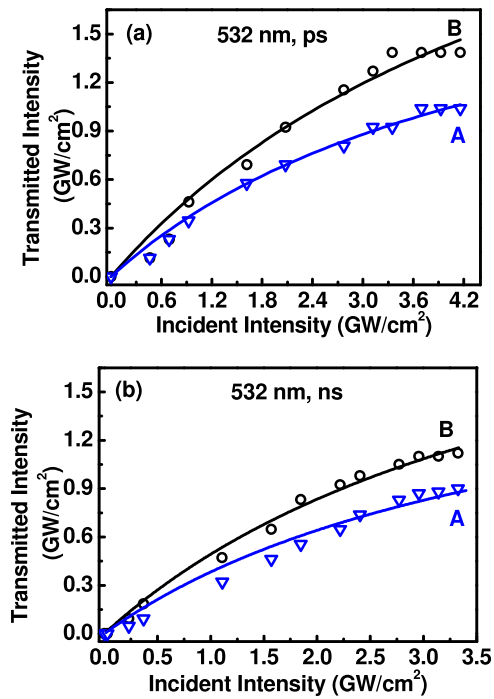


FIG. 3. Transmitted intensity as a function of the incident laser intensity. Excitation at 532 nm with laser pulses of 80 ps (a) and 250 ns bursts of 80 ps pulses (b). The solid lines represent fits of Eq. (4) to the experimental points.

B. Picosecond and nanosecond experiments at 532 nm

NL transmittance experiments were performed using the second harmonic of a mode-locked and Q-switched Nd:YAG laser (532 nm). The NL behavior of the samples at 532 nm is illustrated in Fig. 3 that shows the transmitted intensity through the samples as a function of the input laser intensity. The incident intensity was controlled using a $\lambda/2$ waveplate followed by a glan-prism that determines the linear polarization of the exciting laser beam arriving in the sample. The incident and transmitted intensities were detected using silicon photodiodes after attenuation with calibrated filters. Fig. 3(a) was obtained with single 80 ps pulses at 6 Hz, while Fig. 3(b) was obtained using bursts of ≈ 20 pulses of 80 ps at

6 Hz. In both cases, it is clear that a deviation from the linear behavior indicates NL absorption of the incident beam.

To determine the NL parameters of the samples, we described the laser propagation along the z direction by

$$\frac{dI(z)}{dz} = -\alpha_0 I(z) - \alpha_2 I^2(z) - \sigma_{FC} N I(z), \quad (1)$$

where $I(z)$ is the beam intensity at the position z inside the sample in a given instant, α_0 is the linear absorption coefficient, α_2 is the TPA coefficient, N is the photogenerated free-carriers density, and σ_{FC} is the free-carriers absorption cross-section. The entrance and exit faces of the sample correspond to $z = 0$ and $z = d$, respectively.

The free-carriers density is governed by the equation

$$\frac{dN}{dt} = \left[\frac{\alpha_0}{\hbar\omega} + \frac{\alpha_2 I(z, t)}{2\hbar\omega} \right] I(z, t), \quad (2)$$

where $\hbar\omega$ is the photon energy. A term related to the free-carriers relaxation time, τ_N , was not included in Eq. (2) because we assumed that $\tau_N > 250$ ns.

For experiments with single pulses, the system of equations (1) and (2) has the analytical solution given in Ref. 7 that can be applied to describe the results of Fig. 3(a). However, for excitation with bursts of 80 ps pulses with an envelope of 250 ns, we have to consider the successive excitation of free-carriers by each pulse of the burst. The Q-switched burst was represented by $I(z, t) = f(t)I(z)$, where $f(t)$ is the normalized temporal profile of the burst, i.e., the Q-switched Gaussian envelope of about 250 ns FWHM containing ≈ 20 pulses of 80 ps separated by ≈ 13 ns. Equation (2) can be integrated and assumes the form

$$N(z) = \frac{\alpha_0}{\hbar\omega} I(z) \int f(t) dt + \frac{\alpha_2}{2\hbar\omega} I^2(z) \int f^2(t) dt, \quad (3)$$

where the integrals $C = \int f(t) dt$ and $D = \int f^2(t) dt$ can be evaluated numerically. The obtained values were $C = 4.8 \times 10^{-9}$ s and $D = 2.4 \times 10^{-9}$ s. Then, using Eq. (3) to solve Eq. (1), we obtain the intensity transmitted through the sample that is given by the expression

$$I_d = \frac{(1-R)^2 I_0 e^{-\alpha_0 d} [\alpha_0 + (\alpha_2 + \delta) I_d + \gamma I_d^2]^{+0.5} [\alpha_0 + (\alpha_2 + \delta) I_0 (1-R) + \gamma I_0^2 (1-R)^2]^{-0.5}}{\left(\frac{\sqrt{\Delta} + (\alpha_2 + \delta) + 2\gamma I_d \sqrt{\Delta} - (\alpha_2 + \delta) - 2\gamma I_0 (1-R)}{\sqrt{\Delta} - (\alpha_2 + \delta) - 2\gamma I_d \sqrt{\Delta} + (\alpha_2 + \delta) + 2\gamma I_0 (1-R)} \right)^{(\alpha_2 + \delta)/2\sqrt{\Delta}}}, \quad (4)$$

where d is the sample thickness, R is the reflectance of each sample-air interface, $I_0 = I(z = 0)$, $I_d = I(z = d)$, $\Delta = (\alpha_2 + \delta)^2 - 4\alpha_0\gamma$, $\delta = C(\alpha_0 \sigma_{FC}/\hbar\omega)$, and $\gamma = D(\alpha_2 \sigma_{FC}/2\hbar\omega)$. Equation (4) has the same form of the expression (3) presented in Ref. 7 for excitation with single pulses, but here, it contains information about the Q-switched and mode-locked pulse train through the parameters δ and γ . Equation (4) is valid for arbitrary values of I_0 .

For low intensities and single pulse excitation, it agrees with the result presented in Ref. 28. Notice that Eq. (4) has two independent parameters, α_2 and σ_{FC} , that can be determined from the best fitting of Eq. (4) to the experimental data.

The data obtained in the 80 ps experiments, shown in Fig. 3(a), were fitted choosing $\sigma_{FC} = 0$, in accordance with our expectation that free-carriers absorption does not play an

important role in the experiments with single 80 ps pulses. The α_2 values obtained are indicated in Table II.

To analyze the results of the 250 ns experiments, the values of α_2 determined in the 80 ps experiments were used, and a data fitting was performed to obtain the values of σ_{FC} . It is important to remark that the results of Fig. 3(b) for 250 ns excitation could not be fitted with $\sigma_{FC} = 0$. The σ_{FC} values, indicated in Table II, are the best values obtained using the software MATHCAD.

The calculated results for both excitation conditions are represented by the solid lines in the Figs. 3(a) and 3(b).

Notice that the NL absorption parameters measured at 532 nm have the same order of magnitude than for typical semiconductors^{29,30} and indicate that the BGO glass can be used for optical limiting in the pico- and nanosecond regimes.

IV. SUMMARY

In the present work, we analyzed the NL behavior of Bi₂O₃-GeO₂ glass at 532 nm and 800 nm for two relative concentrations of the constituents' compounds. The results show that this material presents large two-photon absorption at 532 nm and is a good candidate for optical limiting in the picosecond and nanosecond regimes. On the other hand, BGO glass presents ultrafast optical response, high refractive nonlinearity, and low nonlinear absorption at 800 nm, but it seems not competitive for all-optical switching in the femtosecond regime.

ACKNOWLEDGMENTS

Financial support by the Fundação de Amparo à Ciência e à Tecnologia do Estado de Pernambuco (FACEPE) and the Conselho Nacional de Desenvolvimento Científico e Tecnológico (CNPq) through the National Institute of Photonics (INCT Project) is acknowledged.

¹M. Yamane and Y. Asahara, *Glasses for Photonics* (Cambridge University Press, Cambridge, UK, 2000).

²S. Smolorz, I. Kang, F. Wise, B. G. Aitken, and N. F. Borrelli, *J. Non-Cryst. Solids* **256–257**, 310 (1999).

³R. L. Sutherland, *Handbook of Nonlinear Optics* (Marcel Dekker, Inc., 2003).

⁴R. A. H. El-Mallawany, *Tellurite Glasses Handbook: Physical Properties and Data* (CRC, 2002).

⁵B. L. You, A. B. Bykov, T. Qiu, P. P. Ho, R. R. Alfano, and N. Borrelli, *Opt. Commun.* **215**, 407 (2003).

⁶F. El-Diasty and M. Abdel-Baki, *J. Appl. Phys.* **106**, 053521 (2009).

⁷T. R. Oliveira, L. de S. Menezes, and C. B. de Araújo, *Phys. Rev. B* **76**, 134207 (2007).

⁸T. R. Oliveira, L. de S. Menezes, E. L. Falcão-Filho, A. S. L. Gomes, C. B. de Araújo, K. Sakaguchi, F. P. Mezzapesa, I. C. S. Carvalho, and P. G. Kazansky, *Appl. Phys. Lett.* **89**, 211912 (2006).

⁹D. Manzani, C. B. de Araújo, G. Boudebs, Y. Messaddeq, and S. J. L. Ribeiro, *J. Phys. Chem. B* **117**, 408 (2013).

¹⁰G. Poirier, C. B. de Araújo, Y. Messaddeq, S. J. L. Ribeiro, and M. Poulain, *J. Appl. Phys.* **91**, 10221 (2002).

¹¹J. Ren, G. Dong, S. Xu, R. Bao, and J. Qiu, *J. Phys. Chem. A* **112**, 3036 (2008).

¹²M. Peng, J. Qiu, D. Chen, X. Meng, I. Yang, X. Jiang, and C. Zhu, *Opt. Lett.* **29**, 1998 (2004).

¹³X. Tiefeng, C. Feifei, D. Shixun, N. Qiuhua, S. Xiang, and W. Xunsi, *Physica B* **404**, 2012 (2009).

¹⁴T. Xu, F. Chen, S. Dai, Q. Nie, X. Shen, and X. Wang, "Femtosecond measurement of third-order optical nonlinearities in Bi₂O₃-B₂O₃-BaO glasses," *Chin. Opt. Lett.* **8**, 70 (2010).

¹⁵T. Xu, F. Chen, S. Dai, X. Shen, X. Wang, Q. Nie, C. Liu, K. Xu, and J. Heo, "Glass formation and third-order optical nonlinear properties within TeO₂-Bi₂O₃-BaO pseudo-ternary system," *J. Non-Cryst. Solids* **357**, 2219 (2011).

¹⁶M. J. Weber and R. R. Monchamp, *J. Appl. Phys.* **44**, 5495 (1973).

¹⁷X. Jiang, X. Guo, H. Tang, X. Fan, Y. Zhan, Q. Wang, L. Zheng, H. Li, and J. Xu, *Opt. Lett.* **37**, 4260 (2012).

¹⁸X. Guo, H. J. Li, L. B. Su, P. S. Yu, H. Y. Zhao, J. F. Liu, and J. Xu, *Laser Phys.* **21**, 901 (2011).

¹⁹L. R. P. Kassab, A. de O. Preto, W. Lozano, F. X. de Sá, and G. S. Maciel, *J. Non-Cryst. Solids* **351**, 3468 (2005).

²⁰B. K. S. P. Singh, *Bismuth Oxide and Bismuth Oxide Doped Glasses for Optical and Photonic Applications* (Nova Science Publishers, Inc., New York, 2012).

²¹Th. Maeder, *Int. Mater. Rev.* **58**, 3 (2013).

²²M. Peng, B. Wu, N. Da, W. Chen, and D. Chen, *J. Non-Cryst. Solids* **354**, 1221 (2008).

²³I.-I. Oprea, H. Hesse, and K. Betzer, *Opt. Mater.* **26**, 235 (2004).

²⁴T. Hasegawa, *J. Non-Cryst. Solids* **357**, 2857 (2011).

²⁵V. Dimitrov and T. Komatsu, *J. Solid State Chem.* **163**, 100 (2002).

²⁶S. Couris, M. Renard, O. Faucher, B. Lavorel, R. Chauv, E. Koudoumas, and X. Michaut, *Chem. Phys. Lett.* **369**, 318 (2003).

²⁷F. Yoshino, S. Polyakov, and G. I. Stegeman, *Appl. Phys. Lett.* **84**, 5362 (2004).

²⁸S. Cherukulappurath, J. L. Godet, and G. Boudebs, *J. Nonlinear Opt. Phys. Mater.* **14**, 49 (2005).

²⁹A. A. Said, M. Sheik-Bahae, D. J. Hagan, T. H. Wei, J. Wang, J. Young, and E. W. van Stryland, *J. Opt. Soc. Am B* **9**, 405 (1992).

³⁰K. Tanaka, *J. Phys. Chem. Solids* **68**, 896 (2007).